Proc. Natl. Acad. Sci. USA
Vol. 94, pp. 14590–14595, December 1997
Genetics

Loss of *p21* increases sensitivity to ionizing radiation and delays the onset of lymphoma in *atm*-deficient mice

Y. Alan Wang, Ari Elson*, and Philip Leder†

Department of Genetics, Harvard Medical School, Howard Hughes Medical Institute, 200 Longwood Avenue, Boston, MA 02115

Contributed by Philip Leder, October 27, 1997

ABSTRACT **Ataxia telangiectasia (AT) is an autosomal recessive disorder characterized by growth retardation, cerebellar ataxia, oculocutaneous telangiectasias, and a high incidence of lymphomas and leukemias. In addition, AT patients are sensitive to ionizing radiation. *Atm*-deficient mice recapitulate most of the AT phenotype. $p21^{cip1/waf1}$ (p21 hereafter), an inhibitor of cyclin-dependent kinases, has been implicated in cellular senescence and response to γ-radiation-induced DNA damage. To study the role of p21 in ATM-mediated signal transduction pathways, we examined the combined effect of the genetic loss of *atm* and *p21* on growth control, radiation sensitivity, and tumorigenesis. As might have been expected, our data provide evidence that p21 modifies the *in vitro* senescent response seen in AT fibroblasts. Further, it is a downstream effector of ATM-mediated growth control. In addition, however, we find that loss of *p21* in the context of an *atm*-deficient mouse leads to a delay in thymic lymphomagenesis and an increase in acute radiation sensitivity *in vivo* (the latter principally because of effects on the gut epithelium). Modification of these two crucial aspects of the ATM phenotype can be related to an apparent increase in spontaneous apoptosis seen in tumor cells and in the irradiated intestinal epithelium of mice doubly null for *atm* and *p21*. Thus, loss of p21 seems to contribute to tumor suppression by a mechanism that operates via a sensitized apoptotic response. These results have implications for cancer therapy in general and AT patients in particular.**

Ataxia telangiectasia (AT) is an autosomal recessive multiorgan disorder that is characterized by progressive cerebellar degeneration, immune deficiencies, growth retardation, premature aging, gonadal abnormalities, and sterility. In addition, AT patients are sensitive to ionizing radiation and manifest an increased incidence of lymphoid tumors (for review, see refs. 1–3). Telangiectasia (dilated blood vessels) appear later in the eyes and on the exposed skin of AT patients. This syndrome also shows multiple cellular defects, which include cellular senescence, cytoskeletal abnormalities, chromosomal instability, hypersensitivity to ionizing radiation, and defective cell cycle regulation response. *ATM*, the gene mutated in AT patients, has been identified through positional cloning (4). The 350-kDa ATM protein is similar to a family of proteins containing a highly conserved carboxy-terminal phospatidylinositol 3 kinase domain. Members of this family are involved in cell cycle regulation, telomere length monitoring, meiotic recombination, and DNA repair (for review, see refs. 1–3). However, despite its homology to lipid kinases, the ATM protein has been shown to possess only a serine-threonine phosphoprotein kinase activity, which is expressed ubiquitously in most tissues examined (13–16).

Mouse models for AT have been created (5–8) that recapitulate many aspects of the human AT phenotype. *Atm* mutant mice display pleiotropic defects, including growth retardation, gonadal atrophy, B and T cell deficiencies, and lymphoblastic lymphomas. Murine embryonic fibroblasts (MEFs) derived from *atm* null mice show chromosomal instability, require high serum for growth, senesce early in culture, are sensitive to ionizing radiation, and display defective G_1/S cell-cycle checkpoint controls in response to DNA damage (5–8).

The induction of p53 is impaired in AT cells, indicating p53 acts downstream in the ATM signal transduction pathway (1–3). p53 encodes a transcription factor that is activated in response to DNA damage. One of the target genes that is regulated by p53 is the cyclin-dependent kinase inhibitor, *p21*. It is induced by DNA damage in a p53-dependent manner and arrests cell cycle in G_1 when overexpressed (9, 10, 17). p21 induction also has been observed in cell lines undergoing differentiation or senescence *in vitro* (10, 17). p53 and p21 have been implicated in G_1/S checkpoint control in response to ionizing radiation (11, 12, 17). However, the role of p53 and p21 in G_2/M checkpoint control remains to be established. In addition, p21 is shown to be regulated in a p53-independent manner. For example, high levels of p21 expression are detected in intestine, lung, thymus, and testis in *p53* null mice (18). Induction of p21 under oxidative stress also operates through a p53-independent pathway (19, 20).

Chronically high levels of p21 have been observed in lymphoblasts derived from AT patients and in *atm*-deficient mouse embryonic fibroblasts (8, 21, 22). These results suggest that p21 may mediate cellular senescence and lymphomagenesis in *atm*-deficient cells. In this report, we examine the effects of loss of *p21* on cellular senescence, sensitivity to ionizing radiation, and lymphomagenesis in *atm* null mice and cell lines.

MATERIALS AND METHODS

Cell Culture. All cells were derived from appropriate matings of mice carrying *p21* and *atm* null alleles (6, 11). To produce MEFs of different genotypic combinations, compound heterozygotes (*atm*/+, *p21*/+) were mated, and timed pregnant females were sacrificed at 14.5–16.5 days postcoitum. Internal organs and heads of embryos were removed and used for Southern blot analysis. Embryonic carcasses were rinsed in iced PBS and minced. The embryonic fragments then were digested in trypsin and DNase1. The dissociated cells were then washed in PBS and plated in 10% fetal calf serum in DMEM.

Southern and Western Blot Analyses. Genomic DNA was extracted from embryonic heads, MEFs, and tails and then digested in proteinase K and ethanol-precipitated. Genomic

The publication costs of this article were defrayed in part by page charge payment. This article must therefore be hereby marked "*advertisement*" in accordance with 18 U.S.C. §1734 solely to indicate this fact.

Abbreviations: AT, ataxia telangiectasia; MEF, murine embryonic fibroblast; BrdUrd, 5-bromodeoxyuridine.

*Present address: Department of Molecular Genetics, Weizmann Institute of Science, Rehovot, Israel 76100.
†To whom reprint requests should be addressed. e-mail: leder@rascal.med.harvard.edu.

DNA then was digested with *Eco*RI and separated on a 1% agarose gel. Genomic DNA was blotted onto nylon membranes and hybridized to *atm* and *p21* probes (6, 11). To analyze *p21* expression, 50,000 MEF cells of each different genotype were collected and extracted in RIPA buffer (50 mM Tris·HCl. pH 7.4/1% Nonidet P-40/0.25% Na-deoxycholate/150 mM NaCl/1 mM EDTA/1 mM Na_3VO_4/1 mM NaF/1 μg/ml of aprotinin, leupeptin, and pepstatin). Cell suspensions were collected by centrifugation to remove cellular debris. Protein-containing extracts were mixed with equal volumes of 2× SDS buffer and loaded on a 15% SDS-polyacrylmide gel. After electrophoresis, the gel was semi-dry-transferred to a poly(vinylidene difluoride) membrane and blotted with p21 polyclonal antibody (Oncogene Science). Signal was detected with ECL chemiluminescence (Amersham). The membrane was stripped and reprobed with β-actin antibody (Sigma) under similar conditions.

Cell Proliferation and Saturation Density Assays. MEFs (2×10^4) were triplicate-plated in a series of 35-mm dishes in DMEM containing 10% fetal calf serum. The cultures were maintained for up to 10 days. MEFs were trypsinized and counted in a hemocytometer, and new medium was added to the rest of the plates each day. Passage 4 MEFs were used.

Cell Cycle Analysis. Asynchronized passage 2–3 MEFs in suspension medium were irradiated from a ^{137}Cs source (Astrophysics Research, Long Beach, CA at 99 KV, 5 mA) at a dose rate of 2 Gy/min, replated in 10% fetal calf serum DMEM for 14 hr, and then pulsed with 10 μM 5-bromodeoxyuridine (BrdUrd) for 4 hr. Cells then were fixed in 70% ethanol. For G_0-synchronization, asynchronous cells at 70% confluency were serum-starved for 96 hr in DMEM containing 0.5% fetal calf serum. Cells then were released into growth media for 24 hr with 65 μM BrdUrd. Subsequent fixation of cells was as above. Fixed cells were washed in PBS and treated with 0.1 N HCl containing 0.7% Triton X-100 to denature DNA. Cells then were incubated with anti-BrdUrd antibody (Becton–Dickson) and counterstained with propidium iodide containing RNase A. Replicative DNA synthesis and DNA content were analyzed by FACScan by using CellQuest software. DNA content also was obtained by analyzing data in Modfit LT software.

Radiation Sensitivity. Mice of different genotypes at age 35–40 days were irradiated with 8 Gy or 10 Gy at a dose of 2.03 Gy/min with a ^{137}Cs source (Mark 1 Irradiator, J. L. Shepherd & Sons, San Bernardino, CA). Mice subsequently were housed together and examined daily for clinical symptoms.

Histology. Mouse tissues or tumors were dissected, fixed in Optimal Fix (American Histology Regent, Lodi, CA), dehydrated, embedded in paraffin, sectioned to 7 μm, and stained with haematoxylin and eosin. Tissue images were obtained with a Sony digital camera and analyzed by a pathologist.

RESULTS

Loss of *p21* Rescues Cellular Senescence but Not the G_1/S Checkpoint Defect in *atm*-Deficient Fibroblasts. *Atm*-deficient fibroblasts senesce early in culture and show increased levels of p21 (7, 8, 22). To study the role of p21 in ATM-mediated signal transduction pathways and in aspects of the *atm* phenotype, we generated mice and MEFs that were doubly null for *atm* and *p21*. A total of 58 primary MEF cell lines were derived from doubly heterozygotic matings. Among the anticipated genotypic combinations, four MEF cell lines deficient for both ATM and p21 were identified by Southern blot analysis. As shown in Fig. 1*a*, p21 protein levels are higher in *atm* null MEFs than in wild-type MEFs, whereas—as expected—p21 protein is absent from *p21* null and *atm/p21* double-null MEFs. The growth properties of these MEFs were examined in early passage cells (passage 4) (Fig. 1*b*). Consistent with earlier observations, *atm* null MEFs appear senescent and grow poorly. By contrast, *p21* null MEFs grow rapidly and are contact-inhibited only at high density. As shown in Fig. 1*b*, the loss of p21 in an *atm* null background dramatically alleviates the growth suppressive phenotype of the *atm* null cells. The growth rate of *atm/p21* double-null cells is comparable to that of wild-type cells and saturates at a similar density. In contrast to the early senescent behavior of the *atm* null cells, *atm/p21*

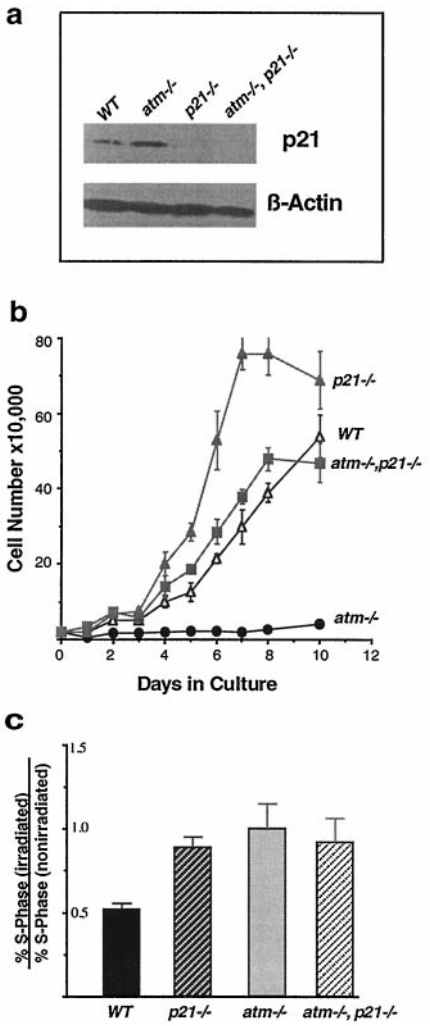

FIG. 1. Cell proliferation and cell cycle analysis. (*a*) Western blot analysis of cell lines used in this study. Lane 1, wild-type MEF cells. Lane 2, *atm* null MEF cells. Lane 3, *p21* null MEF cells. Lane 4, *atm/p21* double-null MEF cells. Increased expression of p21 is seen in *atm* null as compared with wild-type cells. p21 expression is not seen in both *p21* null and *atm/21* double-null cells. A β-actin control for equal loading also is shown. (*b*) Saturation densities and growth properties of the MEFs. MEFs (2×10^4) at passage 4 were plated in triplicate on 35-mm culture dishes, and medium was changed every day. The cell number at each time point represents the mean value of triplicates with an error bar showing standard deviation. The genotype of each cell line is indicated. *atm/p21* double-null cells grow at a similar rate to wild type but slower than *p21* null cells and also arrest at a lower saturation density. (*c*) G_1/S checkpoint defect in *atm/p21* double-null MEFs in response to ionizing radiation. Unsynchronized *atm*, *atm/p21*, *p21*, and wild-type MEFs were irradiated at 0 and 10 Gy. Fourteen hours after irradiation, cells were pulsed with 10 μM of BrdUrd for 4 hr. Cells were fixed and stained with anti-BrdUrd antibody and propidium iodide and analyzed by FACS for S-phase and DNA contents. Three independent experiments were performed at the indicated dosage. The ratios of the percentage of irradiated S-phase cells versus the percentage of nonirradiated S-phase cells are presented with error bars showing standard deviations. Solid bar, wild type; dark hatched bar, *p21/p21*; light solid bar, *atm/atm*; light hatched bar, *atm/p21*.

double-null cells do not growth arrest and can be carried beyond passage 20 (data not shown). Thus, loss of p21 in *atm* null MEF alleviates growth arrest, suggesting that p21 plays a role in the senescent behavior observed in AT MEFs, and that p21 acts downstream in growth control regulated by ATM.

Because both *atm* and *p21* single-null cells are defective in their response to DNA damage (8, 11, 12, 23), it is tempting to suspect that p21 exerts its effects on *in vitro* MEF growth via its role in the DNA radiation damage checkpoint. To understand the epistatic relationship between ATM and p21 in DNA-damage response and cell cycle regulation, asynchronously growing early passage cells of *atm* null, *p21* null, *atm/p21* double-null, and wild-type genotypes were irradiated at 10 Gy and analyzed for cell cycle stage by FACS 18 hr after irradiation (Fig. 1*c*). Wild-type cells demonstrated a 50% reduction in S-phase cells, whereas *atm*, *p21*, and *atm/p21* null cells did not show any significant reduction in S-phase cells after irradiation, indicating that the G_1/S checkpoint is defective in these mutant cell lines (Fig. 1*c*). This result suggests that ATM and p21 invoke G_1/S checkpoint control on the same pathway in response to DNA damage induced by ionizing radiation. One also might imagine that radiation-independent DNA damage incurred as a result of the *atm* deficiency (which leads to an increase in p21; Fig. 1*a*) represses cell growth via p21. Thus, loss of p21 relieves cell cycle checkpoint(s) control.

Loss of p21 Leads to Increased Sensitivity to Ionizing Radiation in *atm*-Deficient Mice. AT mice, like AT patients, are sensitive to ionizing radiation and exhibit acute gut cytoxicity (4). In normal irradiated mice, intestinal epithelial cells undergo apoptosis in a p53-dependent manner (24, 25). Interestingly, however, p21 is expressed at high levels in intestinal tissues in a p53-independent manner (18). It was therefore of interest to study the interaction of *atm* and *p21* in radiation-mediated gut toxicity. To do this study, 5-week-old *atm/p21* double-null mice were irradiated at 8 Gy and compared with *atm* null, *p21* null, and wild-type mice of the same age. Loss of *p21* severely exacerbated the acute radiation sensitivity of AT mice. As shown in Fig. 2*a*, 50% of the *atm/p21* double-null mice survived until day 4 postirradiation, whereas a similar fraction of the single-null AT mice survived until day 8. The difference observed is statistically significant when using the Wilcoxon two-sample test assuming nonparametric data and a two-tail *P* value ($P < 0.002$). All of the wild-type and *p21* null mice survived beyond day 12. Indeed, 16 *p21* null mice were followed and only one of these mice died at 14 days postirradiation. All 20 *atm* heterozygotes in the *p21* null background survived beyond 30 days (data not shown).

The accelerated kinetics of acute radiation toxicity observed in the *atm/p21* double-null mice suggest that ATM and p21 normally cooperate in preventing radiation-induced apoptosis in the intestinal epithelium. To demonstrate that p21 plays a role in protecting intestinal epithelial cells from radiation-induced apoptosis, we irradiated a group of *p21* null mice at 10 Gy and observed that 50% of *p21* null mice succumbed by day 13, whereas all of the wild-type mice survived (Fig. 2*b*). In a separate experiment designed to study the morphologic manifestations of hypersensitivity to ionizing radiation, five mice each of wild-type, *atm*, *p21*, and *atm/p21* single- and double-null genotypes were irradiated at 8 Gy, and sections of intestine taken at days 2, 3, and 4 were examined histologically. Consistent with the result presented in Fig. 2*a*, all *atm/p21* double-null mice exhibited symptoms of lethargy and malaise as early as 2 days postirradiation, whereas *atm*, *p21* single-null, and wild-type mice appeared to be normal (data not shown). This observation is supported by the increased edematous degeneration seen in *atm/p21* double-null mouse intestinal epithelium and crypts (Fig. 2*f*) as compared with *atm* single null (Fig. 2*e*). In contrast, the intestines of *p21* null mice (Fig. 2*d*) exhibit only minor signs of edematous degeneration of the normal architecture, whereas wild-type intestines (Fig. 2*c*) are entirely normal. This result suggests that ATM and p21 cooperate to prevent radiation-induced apoptosis.

Loss of *p21* Delays the Onset of Lymphoma in *atm*-Deficient Mice. Early studies in p21-deficient mice suggest that p21 does not behave as a tumor suppressor *in vivo*, tumor incidence in these mice being no different than in wild type (11). Nevertheless, the finding of chronically higher levels of p21 in lymphoblasts derived from AT patients (21) suggested an interaction, likely indirect, between these genes. Accordingly, we wanted to assess the role of p21 deficiency on the highly increased incidence of lymphoma in AT mice. Mice of all possible *atm/p21* genotypes were bred and observed for tumor

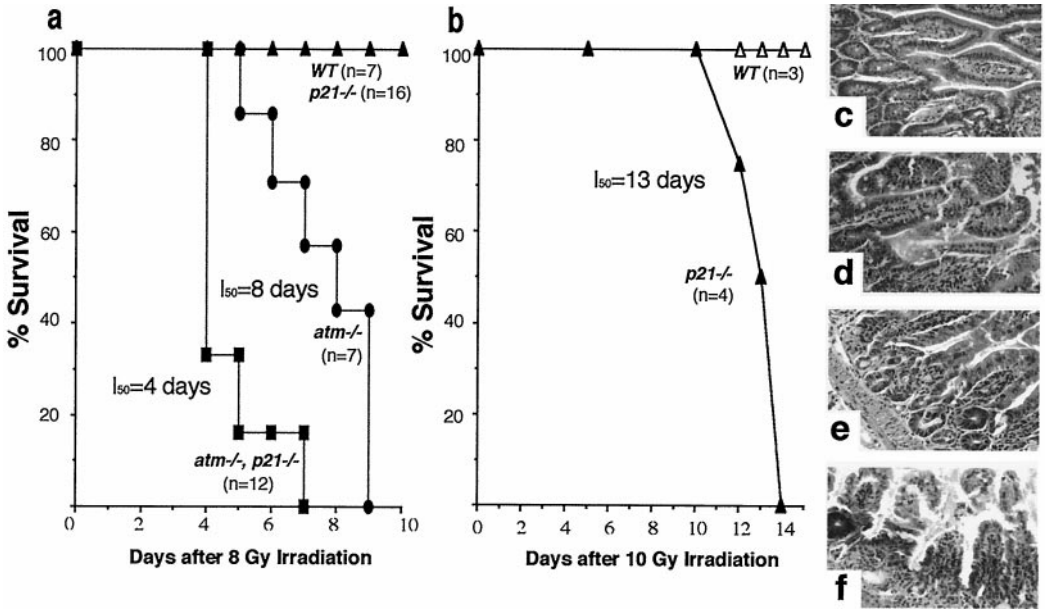

FIG. 2. Acute radiation hypersensitivity in *atm/p21* double-null mice. Survival curves are shown of mice irradiated at (*a*) 8 Gy and (*b*) 10 Gy. Statistical analysis was performed by using Wilcoxon two-sample test assuming nonparametric data and a two-tailed *P* value ($P < 0.002$). Genotypes of mice are indicated. Data in *a* are combined from two separate sets of experiments. Hematoxylin and eosin-stained sections of the small intestine taken at day 3 after 8 Gy irradiation are shown in *c-f* at ×40 magnification. (*c*) Wild type. (*d*) *p21*/null. (*e*) *atm*/null. (*f*) *atm/p21* double null. p21 null mice irradiated at 10 Gy show edematous degeneration of small intestine 3 days postirradiation (data not shown).

formation (largely thymic lymphomas). Interestingly, loss of p21 led to a greater than 50-day delay in the onset of lymphomas in AT mice. As shown in Fig. 3, 50% of the *atm* null mice developed tumors and died by 100 days of age, whereas 50% of mice deficient in both ATM and p21 survived beyond 157 days. Surprisingly, loss of *p21* had a suppressive effect on tumor formation. Pathologic examination of the thymomas themselves provides a strong hint as to the basis of the potential effect of p21 loss. Thymomas derived from *atm/p21* double-null mice show high levels of apoptotic cells in the tumor (n = 4 mice), whereas apoptotic cells are not observed in tumor samples from *atm* null mice (n = 7 mice) (Fig. 4 *a* and *b*). The apoptotic cells in the tumors were confirmed by direct FACS analysis of tumor samples stained with annexin V and propidium iodide (data not shown).

Our studies suggest that a normal function of p21 may be to protect thymic tumor cells against apoptosis and that loss of p21 potentiates the apoptotic response induced by intrinsic or extrinsic means. To test this notion more directly, thy1 positive tumor cell lines were derived from the thymic lymphomas of both *atm* and *atm/p21* null mice to test their propensity to undergo apoptosis spontaneously *in vitro*. Consistent with the *in vivo* finding, an *atm/p21* double-null thymoma cell line showed increased spontaneous apoptosis in comparison to an *atm* thymoma cell line (17% vs. 7%, Fig. 4*c*). A dose- and time-dependent study of the radiation response of these cell lines also was performed. Both *atm* and *atm/p21* thymoma cell lines showed defective G_1 checkpoint control after irradiation at 20 Gy (5 Gy and 10 Gy data not shown) as analyzed by FACS (Fig. 4*c*). Interestingly, the *atm* cell lines exhibited a normal G_2 arrest in a dose- and time-dependent manner, whereas *atm/p21* cell lines lack this G_2 arrest (Fig. 4*c*). The consequence of such a lack of G_2 arrest is the dramatic increase in apoptosis observed at 24 hr postirradiation in the *atm/p21* lymphoma cells (49% vs. 18% in *atm* lymphoma cells).

DISCUSSION

Chronically high levels of p21 expression have been observed in AT lymphoblasts and *atm*-deficient murine fibroblast cell lines (8, 21, 22). These results suggested that p21 might mediate

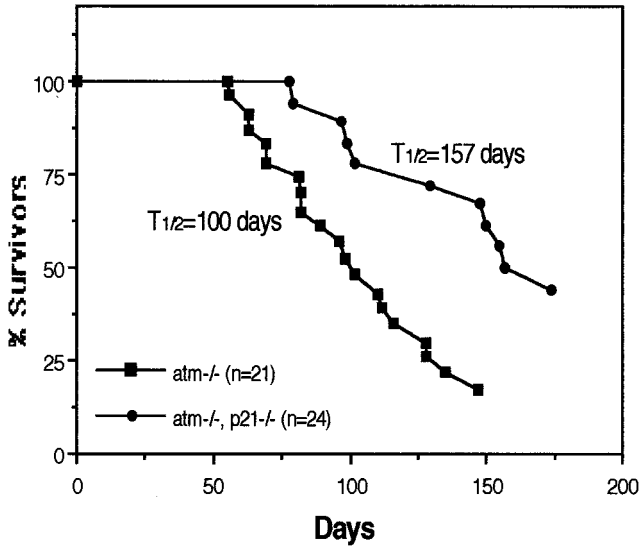

FIG. 3. *atm/p21* double-null mice show delayed tumorigenesis. Tumor-free mouse survival curves are shown. Genotypes and numbers of mice are indicated. Fifty percent of the *atm* null and *atm/p21* double-null mice die before the ages of 100 and 157 days, respectively. Most of the *atm* and *atm/p21* mice died of thymic lymphoma. None of the p21 null (n = 7) and wild-type (n = 16) mice became ill at the indicated times.

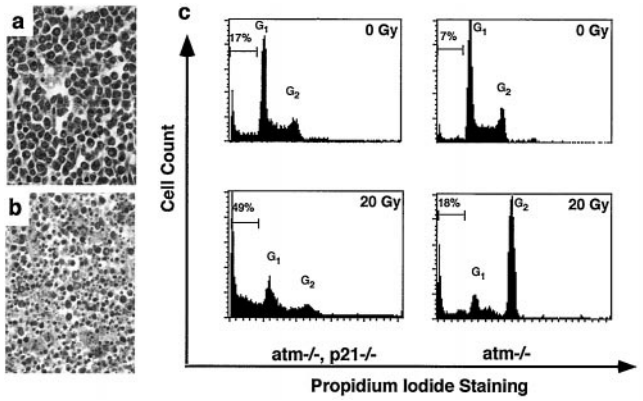

FIG. 4. *atm/p21* double-null tumors exhibit increased apoptosis. (*a* and *b*) Hematoxylin and eosin staining of tumor section. ×40 magnification. (*a*) An *atm* thymic lymphoma shows uniform T lymphoblastic cells with no detectable signs of apoptosis. (*b*) An *atm/p21* double-null thymic lymphoma shows extensive apoptosis. (*c*) DNA damage-induced defective G_2/M checkpoint control in *atm/p21* double-null thymomas leads to increased apoptosis in thymic tumor cells. Tumor cell lines were irradiated at 0 and 20 Gy. Cells were collected at 24 hr, fixed and stained with propidium iodide, and analyzed for DNA content and apoptotic cells. G_1 and G_2 peaks are indicated as well as percentage of apoptotic cells. Similar observations were seen at 5 and 10 Gy of irradiation and from independent cell lines (not shown).

cellular senescence, lymphomagenesis, and other features of the AT phenotype. To examine the role of p21 in ATM-mediated signal transduction pathways, we have used *atm* null mice and cell lines to analyze the effects of loss of p21 on the cardinal features of the AT phenotype. Not surprisingly, given the role p21 plays in cell cycle checkpoint control, we observed that loss of p21 could rescue cellular senescence in *atm*-deficient fibroblast growth in culture. Quite surprisingly, however, we observed that double-null mice exhibited an increased hypersensitivity to ionizing radiation and a striking delay of the onset of tumorigenesis.

Increased cellular levels of p21 are associated with terminal differentiation and cellular senescence (10). In addition, induced p21 expression can be seen under conditions of DNA damage and oxidative stress (19, 20, 26). Atm-deficient fibroblasts grown in culture show severe proliferative defects and senesce. These effects are correlated with an elevated level of p21 (8, 22). Here we have shown that genetic deletion of *p21* in an *atm*-deficient background can rescue cells from senescence and overcome the growth arrest seen in *atm* null fibroblasts. This result indicates that p21 is a key regulator of cellular senescence and that p21 acts downstream in ATM-mediated growth regulation. Although loss of p21 rescues growth deficiency seen in *atm* null cell lines, it is important to point out that *p21* null fibroblasts grow faster and saturate at a higher density than *atm* and *p21* double-null cell lines (Fig. 1*b*). This result suggests that additional growth inhibitors may cooperate with p21 to mediate the growth suppression seen in *atm* null fibroblasts. Our data are consistent with results that showed that genetic deletion of *p53* in the *atm* null background suppresses growth arrest in *atm*-deficient fibroblasts and suggested that this suppression might be because of loss of p21 expression (22). Because a similar growth rate was observed between *p53* single-null and *p53/atm* double-null cell lines (22), it is possible that the expression of additional growth inhibitors besides p21 are suppressed by the loss of p53 in the *atm* null cell lines (22). In addition, our notion that p21 is a central mediator *in vitro* of cellular senescence is supported by the recent observation that genetic deletion of *p21* bypasses cellular senescence in a human diploid fibroblast cell line (27).

Atm null fibroblasts show multiple defects in cell cycle checkpoints. Indeed, one of the hallmarks of the AT phenotype is radioresistant-DNA synthesis (1–3). *p21* null fibroblasts also exhibit radioresistant DNA synthesis and defective G_1/S checkpoint control (11, 12). The availability of mice and cells selectively deficient in both of these genes has allowed us to examine the epistatic relationship between *atm* and *p21* in response to DNA damage and cell cycle regulation. *Atm* and *p21* double-null fibroblasts show a G_1/S checkpoint defect in response to ionizing radiation that is similar to that seen in *atm* or p21 single-null fibroblasts. Our data further indicate that the *atm*- and *p21*-mediated G_1/S checkpoint control pathways are overlapping. It has been demonstrated that the DNA damage checkpoint pathways induced by UV are intact in AT cell lines (3), whereas p21 has been implicated in the regulation of UV-induced DNA damaged checkpoint pathway (26). Accordingly, we find that *atm* and *p21* double-null fibroblasts show G_1/S checkpoint defects that are seen in *p21* null cells, but not in *atm* null cells (data not shown).

Atm null mice show growth retardation at weaning that persists through adult life (5–8). *Atm* and *p21* double-null mice also show growth retardation with about a 30% reduction of body weight as compared with wild-type mice and *p21* null mice (data not shown). Thus, loss of p21 in *atm*-deficient mice does not rescue the growth retardation phenotype. Loss of *atm* also leads to infertility in both male and female mice (5, 6, 8). It was shown that infertility is caused by defects in spermatogenesis and oogenesis. Histological examination of ovaries and testis from *atm*/*p21* double-null reveal defects that are similar to those seen in *atm* null mice, with absence of mature spermatids and degeneration of spermatocytes in testis and missing primary oocytes and follicles in ovaries (data not shown). In addition, we do not observe any overt ataxia in *atm* and *p21* double-null mice, although ataxia is a profound phenotype seen in AT patients.

Atm-deficient mice, like AT patients, are sensitive to ionizing radiation and exhibit acute gut cytoxicity (5). The earliest lethal *in vivo* effects of ionizing radiation are largely caused by toxic effects on the intestinal epithelium. In normal irradiated mice, intestinal epithelial cells undergo apoptosis in a p53-dependent manner (24, 25). Interestingly, *atm*/*p53* double-null mice exhibit a level of gut toxicity that is similar to that of *atm* null mice (28), invoking a different cytotoxic pathway that is p53-independent. It was shown previously that high levels of p21 expression can be detected in intestinal tissue, with the expression being independent of p53 (18). Because radiation hypersensitivity is a serious and confounding feature of AT, it was important to assess the role of p21 in this response. Our results show that *atm*/*p21* double-null mice are more sensitive to ionizing radiation than *atm* single-null mice ($P < 0.002$). This finding is supported further by histologic analysis of irradiated intestinal tissues in which progressively more severe intestinal degeneration is seen in *atm*/*p21* double-null mice than in *atm* single-null mice. Our results suggest that ATM and p21 might cooperate to suppress radiation-induced apoptosis in the intestinal epithelium. It has been suggested that intestinal epithelial cells, in particular crypt cells, arrest cell cycle progression in the G_2 phase in response to ionizing radiation (24). It is conceivable that ATM and p21 might be involved in the G_2/M checkpoint control in the intestinal epithelial cells. Loss of *atm* or *p21* in intestinal epithelial cells would abolish the G_2/M checkpoint control and lead to increased apoptosis in response to ionizing radiation. This hypothesis might be the basis of the increased radiation sensitivity seen in *atm*/*p21* double-null mice.

Recent studies have shown that loss of *atm* in conjunction with loss of *p53* accelerates lymphomagenesis in double-null (as compared with single-null) mice (28). Mice genetically deficient in *p21* (unlike *p53*-deficient mice) are not tumor prone, suggesting that the tumorigenic effect of loss of *p53* might occur through loss of the p53-dependent apoptotic pathway. In addition, elevated levels of p21 are observed in AT lymphoma cell lines, suggesting an interaction between these genes during lymphomagenesis. Interestingly, we show here that loss of *p21* in *atm* null mice delays the onset of tumor formation. Fifty percent of *atm* null mice develop thymic lymphomas by 100 days of age, whereas the onset of lymphomas is delayed—on average—more than 50 days in *atm*/*p21* double-null mice. Furthermore, we show that the delayed tumorigenesis is accompanied by elevated levels of apoptosis seen in *atm*/*p21* double-null thymomas. Such results suggest that the function of *p21* in some malignant cells might be to block access to an apoptotic pathway. Tumor cell lines derived from either *atm* null mice or *atm*/*p21* double-null mice were examined for the response to DNA damage induced by ionizing radiation. Consistent with the previous observation, *atm* null lymphoma cell lines show defective G_1/S checkpoint control but arrest normally at G_2. Interestingly, G_2 arrest is defective or abolished in *atm*/*p21* double-null lymphoma cell lines. The possible consequence of this loss of G_2 arrest might be the dramatic increase in apoptotic cells we observe postirradiation (Fig. 4*c*). This result suggests that p21 might actively monitor G_2/M checkpoint control in these lymphoma cells. Perhaps not surprisingly, it was shown that colon cancer cell lines deficient for p21 undergo apoptosis in response to DNA damage (29). Although a delayed apoptotic response is seen in p21-deficient colon cancer cells (29), the apoptotic response we observe in *atm*/*p21*-deficient lymphoma cell lines appears to occur earlier. It is thus interesting that in both cases, loss of p21 leads to a DNA damage-induced defect in the G_2/M checkpoint in tumor cell lines (lymphoblastic cells and colon epithelial cells) with subsequent susceptibility to apoptosis. In addition, high levels of p21 protein are associated with chemoresistance in acute myelogenous leukemia (30). The findings that introduction of *p21* antisense oligos induces apoptosis, whereas overexpression of p21 protects against apoptosis *in vitro* (31–33) are consistent with the results presented in this report. It is of interest to note that $p57^{KIP2}$ (a member of the p21 cyclin-dependent kinase inhibitor family) null mice show marked increases in apoptosis in lens epithelial cells (34).

Our results demonstrate that p21 is an essential factor in ATM-mediated growth regulation and cellular senescence. In addition, we have demonstrated that p21 and ATM play distinctive and cooperative roles in checkpoint control and apoptosis in response to DNA damage. A summary of the effects we observe and the potential involvement of apoptotic and cell cycle checkpoint mechanisms are shown in Fig. 5. Loss of *atm* leads to radiation sensitivity and lymphomagenesis, possibly through defective DNA repair or replication. Loss of

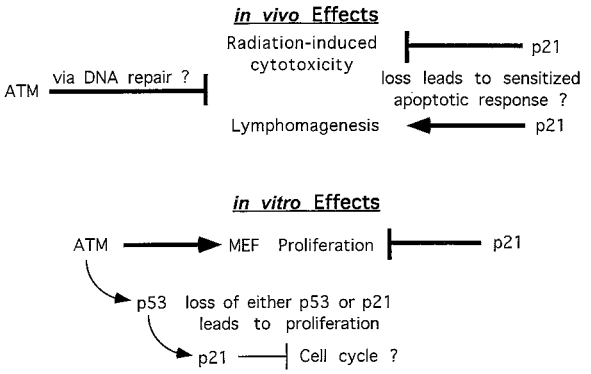

FIG. 5. Summary of *in vivo* and *in vitro* effects of p21 in the context of AT. Arrows indicate inducing effects; blunted arrows indicate inhibitory effects. The indicated effects of p21 are observed in the context of an *atm* null mouse or cell. Statements or pathways followed by a question mark indicate a proposed mechanism. The summary diagram is described in the text.

p21 in this ATM-deficient context stimulates acute radiation sensitivity (intestinal cytoxicity), but delays lymphomagenesis, both possibly by triggering an apoptotic response. Apparently by using a different pathway, p21 relieves the *in vitro* senescent response seen in MEFs, most likely via relief of the G_1/S cell cycle checkpoint. Drugs that specifically inhibit p21 function in cancer cells (or the function of other proteins in its signal pathway), in combination with DNA damaging agents, could lead to more efficient tumor therapy. Our findings provide a framework for further studies relevant to cancer therapy in general and AT patients in particular.

Special thanks go to R. Cardiff for analysis of mouse pathological samples and for helpful suggestions, to B. Leader for help with statistical analysis, to R. Van Etten for instructions in the use of the irradiator, to C. H. Westphal, N. Chester, and Y. Ishida for helpful discussions and comments on the manuscript. Y.A.W. is a Postdoctoral Associate and P.L. is a Senior Investigator of the Howard Hughes Medical Institute. A.E. is an Alon Fellow and incumbent of the Adolfo and Evelyn Blum Career Development Chair in Cancer Research at The Weizmann Institute.

1. Meyn, M. S. (1995) *Cancer Res.* **55,** 5991–6001.
2. Jorgenson, T. J. & Shiloh, Y. (1996) *Int. J. Rad. Biol.* **69,** 527–537.
3. Lavin, M. F. & Shiloh, Y. (1996) *Annu. Rev. Immunol.* **54,** 177–202.
4. Savitsky, K., Bar-Shira, A., Gilad, S., Rotman, G., Ziv, Y., *et al.* (1995) *Science* **268,** 1749–1753.
5. Barlow, C., Hirotsune, S., Paylor, R., Liyanage, M., Eckhaus, M., Collins, F., Shiloh, Y., Crawley, J. N., Ried, T., Tagle, D. & Wynshaw-Boris, A. (1996) *Cell* **86,** 159–171.
6. Elson, A., Wang, Y., Daugherty, C. J., Morton, C. C., Zhou, F., Campos-Torres, J. & Leder, P. (1996) *Proc. Natl. Acad. Sci. USA* **93,** 13084–13089.
7. Xu, Y., Ashley, T., Brainerd, E. E., Bronson, R. T., Meyn, M. S. & Baltimore, D. (1996) *Genes Dev.* **10,** 2411–2422.
8. Xu, Y. & Baltimore, D. (1996) *Genes Dev.* **10,** 2401–2410.
9. el-Deiry, W. S., Tokino, T., Velculescu, V. E., Levy, D. B., Parsons, R., Trent, J. M., Lin, D., Mercer, W. E., Kinzler, K. W. & Vogelstein, B. (1993) *Cell* **75,** 817–825.
10. Harper, J. W. & Elledge, S. J. (1996) *Curr. Opin. Genet. Dev.* **6,** 56–64.
11. Deng, C., Zhang, P., Harper, J. W., Elledge, S. J. & Leder, P. (1995) *Cell* **82,** 675–684.
12. Brugarolas, J., Chandrasekaran, C., Gordon, J. I., Beach, D., Jacks, T. & Hannon, G. J. (1995) *Nature (London)* **377,** 552–557.
13. Chen, G. & Lee, E. (1996) *J. Biol. Chem.* **271,** 33693–33697.
14. Keegan, K. S., Holtzman, D. A., Plug, A. W., Christenson, E. R., Brainerd, E., Flaggs, G., Bentley, N. J., Taylor, E. M., Meyn, M. S., Moss, S. B., Carr, A. M., Ashley, T. & Hoekstra, M. F. (1996) *Genes Dev.* **10,** 2423–2437.
15. Jung, M., Kondratyev, A., Lee, S. A. Dimtchev, A. & Dritschilo, A. (1997) *Cancer Res.* **57,** 24–27.
16. Baskaran, R., Wood, L. D., Whitaker, L. L., Canman, C. E., Morgan, C. E., Xu, Y., Barlow, C., Baltimore, D., Wynshaw-Boris, A., Kastan, M. B. & Wang, J. Y. (1997) *Nature (London)* **387,** 516–519.
17. Elledge, S. J. (1996) *Science* **274,** 1664–1672.
18. Macleod, K. F., Sherry, N., Hannon, G., Beach, D., Tokino, T., Kinzler, K., Vogelstein, B. & Jacks, T. (1995) *Genes Dev.* **9,** 935–944.
19. Russo, T., Zambrano, N., Esposito, F., Ammendola, R., Cimino, F., Fiscella, M., Jackman, J., O'Connor, P. M., Anderson, C. W. & Appella, E. (1995) *J. Biol. Chem.* **270,** 29386–29391.
20. Qiu, X., Forman, H. J., Schonthal, A. H. & Cadenas, E. (1996) *J. Biol. Chem.* **271,** 31915–31921.
21. Beamish, H., Williams, R., Chen, P. & Lavin, M. F. (1996) *J. Biol. Chem.* **271,** 20486–20493.
22. Westphal, C. H., Schmaltz, C., Rowan, S., Elson, A., Fisher, D. E. & Leder, P. (1997) *Cancer Res.* **57,** 1664–1667.
23. Waldman, T., Kinzler, K. W. & Vogelstein, B. (1995) *Cancer Res.* **55,** 5187–5190.
24. Potten, C. S., Owen, G. & Roberts, S. A. (1990) *Int. J. Rad. Biol.* **57,** 185–199.
25. Clarke, A. R., Gledhill, S., Hooper, M. L., Bird, C. C. & Wyllie, A. H. (1994) *Oncogene* **9,** 1767–1773.
26. Elledge, S. J. & Harper, J. W. (1994) *Curr. Opin. Cell Biol.* **6,** 847–852.
27. Brown, J. P., Wei, W. & Sedivy, J. M. (1997) *Science* **277,** 831–834.
28. Westphal, C. H., Schmaltz, C., Rowan, S., Elson, A., Fisher, D. E. & Leder, P. (1997) *Nat. Genet.* **16,** 397–401.
29. Waldman, T., Lengauer, C., Kinzler, K. W. & Vogelstein, B. (1996) *Nature (London)* **381,** 713–716.
30. Zhang, W., Kornblau, S. M., Kobayashi, T., Gambel, A., Claston, D. & Deisseroth, A. B. (1995) *Clin. Cancer Res.* **1,** 1051–1057.
31. Poluha, W., Poluha, D. K., Chang, B., Crosbie, N. E., Schonhoff, C. M., Kilpatrick, D. L. & Ross, A. H. (1996) *Mol. Cell. Biol.* **16,** 1335–1341.
32. Gorospe, M., Wang, X., Guyton, K. Z. & Holbrook, N. J. (1996) *Mol. Cell. Biol.* **16,** 6654–6660.
33. Gorospe, M., Cirilli, C., Wang, X., Seth, P., Capogrossi, C. & Holbrook, N. J. (1997) *Oncogene* **14,** 929–935.
34. Zhang, P., Liegeois, N. J., Wong, C., Finegold, M., Hou, H., Thompson, J. C., Silverman, A., Harper, J. W., DePinho, R. A. & Elledge, S. J. (1997) *Nature (London)* **387,** 151–158.